Document Version
Final published version

Numerical Simulation of the Dynamic Out-Of-Plane Two-Way Bending Seismic Behaviour of Unreinforced Masonry Walls Using Equivalent SDOF Systems

Satyadhrik Sharma[1]([envelope]), Helene Bouwmeester[1], Francesco Graziotti[2], and Francesco Messali[1]

[1] Faculty of Civil Engineering and Geosciences, Technische Universiteit Delft, Stevinweg 1, 2628 CN Delft, The Netherlands
S.Sharma-9@tudelft.nl

[2] Department of Civil Engineering and Architecture—DICAr, Università di Pavia, 27100 Pavia, Italy

Abstract. Damage and collapse of walls in the out-of-plane (OOP) direction are common failure modes in existing unreinforced masonry (URM) buildings when subjected to seismic excitation. These localized mechanisms also hinder the real-isation of the complete in-plane seismic capacity of URM buildings. Among such OOP failures, a distinction can be made between (i) one-way bending which occurs in long walls and walls without side supports, and (ii) two-way bending which occurs in walls that have at least one vertical and one horizontal edge supported. This paper examines the suitability of a single-degree-of-freedom model for modelling the dynamic behaviour of URM walls subjected to OOP seismic excitation and undergoing two-way bending. The model operates in two phases: (i) initial elastic and (ii) post cracking, transitioning instantaneously between the phases once the force required to crack the wall is surpassed. Post cracking, the wall is treated as a system comprised of rigid blocks, and wall resistance is computed by combining three distinct contributions. These contributions are (i) bilinear elastic rigid block rocking, (ii) elastoplastic friction, and (iii) bilinear degrading component taking into account strength and stiffness degradation of walls. The model's complete behaviour in both phases is described by six independent parameters, which can be computed analytically. This paper explores the performance of the proposed model, especially when compared with and calibrated against experimental results from incremental dynamic testing of full-scale single leaf and cavity walls, for which the model demonstrates excellent agreement.

Keywords: Unreinforced masonry · Out-of-plane · Hysteresis model · Single-degree-of-freedom system · Two-way-bending

1 Introduction

In the field of earthquake engineering, the evolution of seismic risk analysis necessitates the development of models that are not only computationally efficient but also possess the ability to accurately predict structural collapse. The vulnerability of unreinforced masonry (URM) structures under seismic action, particularly regarding the out-of-plane (OOP) direction, is widely acknowledged. This has led to the formulation of various analytical approaches targeting the OOP dynamics of URM walls [1–4]. These analytical approaches assess the OOP behaviour of URM, assuming the walls act as collections of either rigid or semi-rigid blocks, based on the premise that the walls are already cracked. This assumption—that walls have pre-existing cracks—is deemed a reasonable approach for one-way vertically spanning walls subjected to unidirectional vertical bending, since their initial crack resistance is generally much lower than the forces needed to initiate a kinematic action, largely due to the masonry's poor tensile strength. However, for two-way spanning walls, research by Graziotti et al. [5] and Sharma et al. [6], via dynamic experiments on full-scale walls, suggests this assumption may be excessively conservative. These walls displayed a pre-cracking resistance substantially above any force that could induce a kinematic mechanism, arguing against their classification as pre-cracked. Thus, this research examines the suitability of a model considering the uncracked state of two-way spanning URM walls for modelling their dynamic OOP response. The model builds upon the work by Vaculik and Griffith [7], who developed OOP load-displacement frameworks for two-way spanning URM walls but overlooked their initial uncracked state. An overview of the experimental data used as a reference in this research is initially outlined in Sect. 2. Following that, the methodology of the newly developed model is detailed in Sect. 3, where guidelines for the analytical determination of model parameters are also provided. Section 4 delves into the model's calibration process and its performance in relation to the experimental benchmarks.

2 Reference Experiments

The reference experiments adopted in this paper are two single leaf and one cavity full-scale URM walls tested incrementally dynamically by Graziotti et al. [5]. These tests were part of a larger experimental campaign that aimed to assess the vulnerability of unreinforced buildings under the action of induced seismicity in Groningen, the Netherlands [8–10]. Both the single leaf walls have the same dimensions, i.e. a length of 4 m and height of 2.75 m. They were also tested with the same boundary conditions, with bottom and lateral edges restrained but the top edge kept free. Fully interlocking 1 m long return walls were constructed along the vertical edges. They were designed to be full moment restraints, thereby functioning as if the restrained edges were completely fixed. What characterizes and makes each single leaf wall unique is the adopted unitmortar combination: 1) wall CS-000-RF was constructed in calcium silicate (CS) brick while 2) wall CL-000-RF was constructed in clay brick (CL) masonry. When these two masonry types are tested under pure horizontal bending, CS brick masonry exhibits vertical line crack and can be therefore classified as a "Weak Unit-Strong Joint" URM typology; on the opposite, saw-toothed stepped cracks develop in CL masonry, being it then classified

as a "Strong Unit-Weak Joint" typology. The cavity wall, CAV-000-RF consisted of a leaf each in both CS and CL masonry connected by metal ties (2 ties/m^2) was also tested in with three edges restrained but the top edge kept free. The CL leaf is the outer leaf and consequently had a marginally longer length of 4.39 m while the inner CS leaf had exactly the same dimensions as CS-000-RF.

    None of the walls show any damage below accelerations up to 1g, indicating significant cracking strength. This large resistance needs to be accounted for while carrying out seismic assessments. Additionally, the effect of the distinct URM material typologies ("Weak Unit-Strong Joint" or "Strong Unit-Weak Joint") was clearly perceived in the failure mechanisms of the walls under dynamic excitation. Due to the formation of line cracks passing through bricks along the vertically restrained edges, CS-000-RF eventually exhibited one-way bending behaviour. The cracks were vertical (as opposed to stepped or saw-toothed), providing negligible frictional resistance (Fig. 1a). In the case of CL-000-RF, two-way bending behaviour was observed following the formation of the crack pattern required for the failure mechanism to develop, with significant frictional resistance contributions from the stepped cracks (Fig. 1b). For CAV-000-RF, the wall ties ensured a sufficient coupling of the horizontal displacement of the two leaves (i.e. limiting the differential displacement and maintaining the gap) up to near collapse. This was due to the axial stiffness and bond of the ties as well as the slenderness of the two leaves. Damage pattern and failure mechanisms observed for the individual wall leaves of CAV-000-RF were very similar to failure mechanisms observed individually for CS-000-RF and CL-000-RF (Fig. 1c).
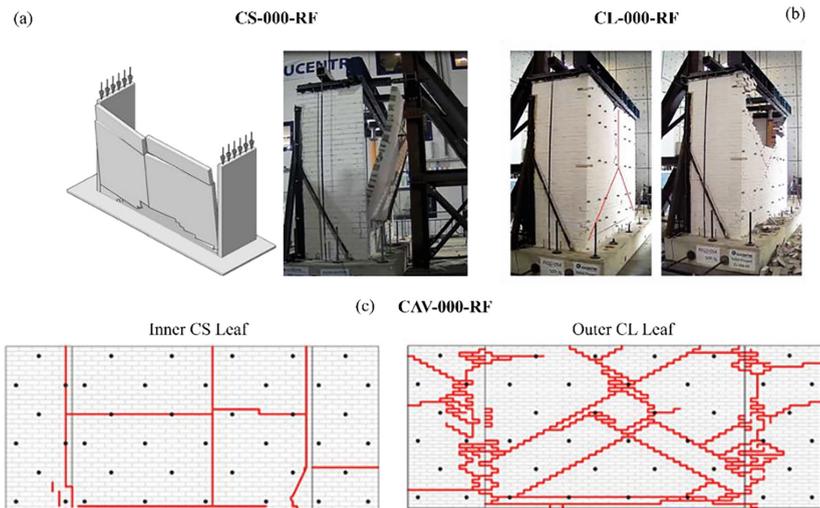

Fig. 1. Failure mechanisms of walls (a) CS-000-RF; (b) CL-000-RF and (c) CAV-000-RF observed experimentally.

3   The Proposed Model

The proposed model functions in two phases:1) initial elastic phase and 2) post crack-ing phase. The initial elastic phase is completely defined by coordinates of the points corresponding to the achievement of the peak strength: *Fcr* (peak strength) and *ucr* (the displacement at which the peak strength is attained) (Fig. 2a). Once *Fcr* is exceeded, the model immediately switches to the post-cracking phase, where the resistance of the walls is modelled via the superposition of three contributing sources:

- A bilinear elastic component, which accounts for rocking (*Fo, uo, uo,f*) (Fig. 2b);
- An elastoplastic component, which takes into account the torsional frictional resistance (*Ffr, ufr*) that develops on the cracked masonry bed joints (Fig. 2c);
- A bilinear component which unloads with secant stiffness, which accounts for the degradation of both the wall strength and stiffness under two-way bending excitation (*Fdeg, udeg, udeg,f*) (Fig. 2d).
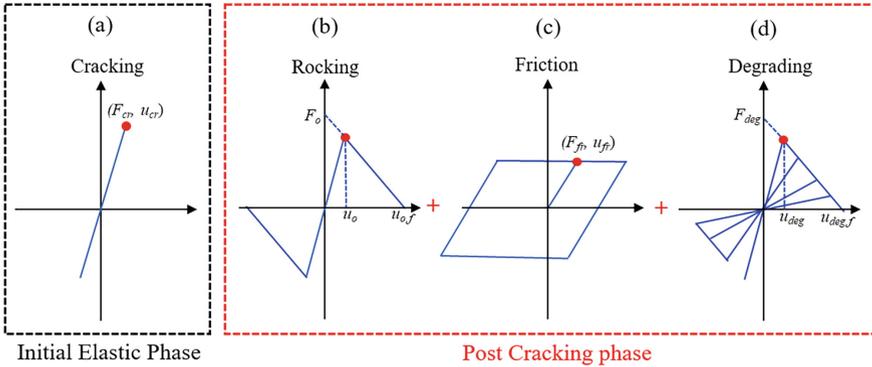

Fig. 2. Schematic representation of the proposed model.

The behaviour of the model is thus governed by a total of 10 input parameters namely: *Fcr, ucr, Fo, uo, uo,f, Ffr, ufr, Fdeg, udeg* and *udeg,f*. However, this reduces to 6 input parameters: *Fcr, ucr, Fo, uo,f, Ffr,* and *udeg,f* due to the assumption that the model shifts instantaneously from the initial elastic phase to post cracking phase on the attainment of *Fcr*. To ensure numerical continuity between these two phases, this assumption translates to:

$$u_{cr} = u_o = u_{fr} = u_{\deg}$$
$$F_{\deg} = F_{cr} - F_o - F_{fr} \tag{1}$$

Physically, Eq. 1 is tantamount to letting the strength and stiffness degradation of URM, rocking and friction along cracked joints start occurring once the strength of the panel has been exceeded and a failure mechanism has been formed. This is not only reasonable but was also experimentally observed in both the reference experimental

campaign Graziotti et al. [5] as well as incremental dynamic testing reported in Sharma et al. [6].

In order to estimate *ucr* (and consequently *uo*, *ufr*, *udeg*), it has been demonstrated in Sharma *et al.*[6] that an analytical formulation based on the theory of plates can be used to calculate the initial stiffness as well as cracking displacement of two-way spanning URM walls under OOP loading. To calculate *Fcr*, *Fo*, *uo* and *Ffr* a failure mechanism needs to be postulated for the wall *a priori*. This can be done based on the boundary conditions and geometry of the wall as per the recommendations provided by Lawrence and Marshall [11], which have been incorporated in the building codes of Australia [12] and the Netherlands [13]. These recommendations, which are based on the virtual work method, can be subsequently used to calculate also *Fcr*. The improved formulations to calculate the moment capacity of cracks proposed by Willis [14], Vaculik [15] and Sharma [16] are employed. For the remaining input parameters controlling the rocking and frictional components in Fig. 2, the mechanics-based formulas developed in Vaculik and Griffith [7] can be adopted.

4   Calibrated Numerical vs. Experimental Performance

The model was subjected to non-linear time-history analysis and calibrated with the experimental tests conducted on the three full-scale walls, as detailed in Sect. 2. These experiments entailed incremental dynamic testing, where a sequence of input motions with gradually increasing intensity was administered to each wall. Typically, following the observation of damage, the incremental testing would recommence at a lower intensity level of the input motions previously applied. The complete series of tests are documented in Graziotti *et al.* [5]. Given the extensive nature of the test sequences, involving over 20 runs for each case, this paper will only discuss the simulation of specific test runs where damage was noted, alongside the tests that immediately preceded and followed those instances.

Initiating the application of the suggested model involves transforming the walls into single-degree-of-freedom (SDOF) systems, which are characterised by an effective mass (*Meff*) and displacement (*Δeff*), which can be calculated with the guidelines set forth by Vaculik and Griffith ([17]). Following this, the SDOF systems that represent the walls underwent incremental dynamic analyses by solving the motion equation (Eq. 2). For these analyses, the Newmark 'linear acceleration' integration method was employed in its non-iterative version [18].

$$M_{eff} \cdot \ddot{u}(t) + C(t) \cdot \dot{u}(t) + f(\dot{u}(t)) = M_{eff} \cdot \ddot{u}_g(t) \qquad (2)$$

Within Eq. 2, time is denoted by t, and the symbols u, $\dot{u}$, $\ddot{u}$ represent the SDOF system's corresponding displacement, velocity, and acceleration, respectively, associated with the wall. The function $f(u, t)$ signifies the restoring force of the wall, which varies depending on the model's current phase (as illustrated in Fig. 2), while $\ddot{u}_g$ stands for the ground acceleration, that is, the input motion being applied in this scenario. The damping coefficient, *C(t)*, was determined based on a constant damping ratio (ξ) ap-plied to the initial circular frequency ($\omega 1$) of the SDOF system. At the onset, in the elastic phase, the model assumes a damping ratio of 0.05. Following the onset of cracking, adjustments

to ξ are made to ensure a calibration with experimental findings. The key parameters of the recommended computational model were initially derived following the analytical guidelines outlined in Sect. 3, subsequently fine-tuned to align the model's numerical outcomes with experimental observations in terms of:

- Force-displacement hysteresis (Fig. 3);
- Displacement time-histories in the simulated tests in the incremental dynamic testing sequence (Figs. 4, 5 and 6).

The calibrated model's performance is demonstrated through the comparision of numerical and experimental force-displacement hysteresis. There is also a notable congruence between the numerical and experimental displacement time histories, underscoring the model's ability to predict collapse scenarios (as depicted in Figs. 4 and 5). The parameters that were adopted to obtain this response are detailed in Table 1. An important observation is that these parameters are set only at the commencement of the test sequence. Following the occurrence of cracking, the stiffness of the component undergoing degradation is dynamically revised, starting from its value at the conclusion of the preceding test run.

Table 1. Calibrated controlling parameters of the proposed model.

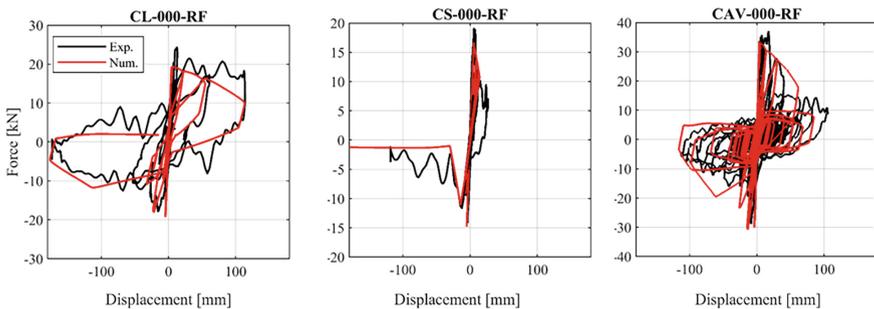| | F_{cr} | u_{cr} | F_o | $u_{o,f}$ | F_{fr} | F_{deg} | $u_{deg,f}$ | ξ |
	[kN]	[mm]	[kN]	[mm]	[kN]	[kN]	[mm]	[–]
CS-000-RF	24.8	5.5	0.91	102	0.3	28.95	30	0.0235
CL-000-RF	29.12	4.4	3.48	204	3.78	22.33	200	0.0205
CAV-000-RF	50	3.4	3.18	102	5.45	42.61	115	0.0244

Fig. 3. Comparison of numerical and experimental force-displacement hysteresis.

5 Concluding Remarks

This paper evaluate the adequacy of a single-degree-of-freedom model for simulating the out-of-plane (OOP) behaviour of unreinforced masonry (URM) walls subject to two-way bending. The model operates in two phases: an initial elastic phase and a sub-sequent
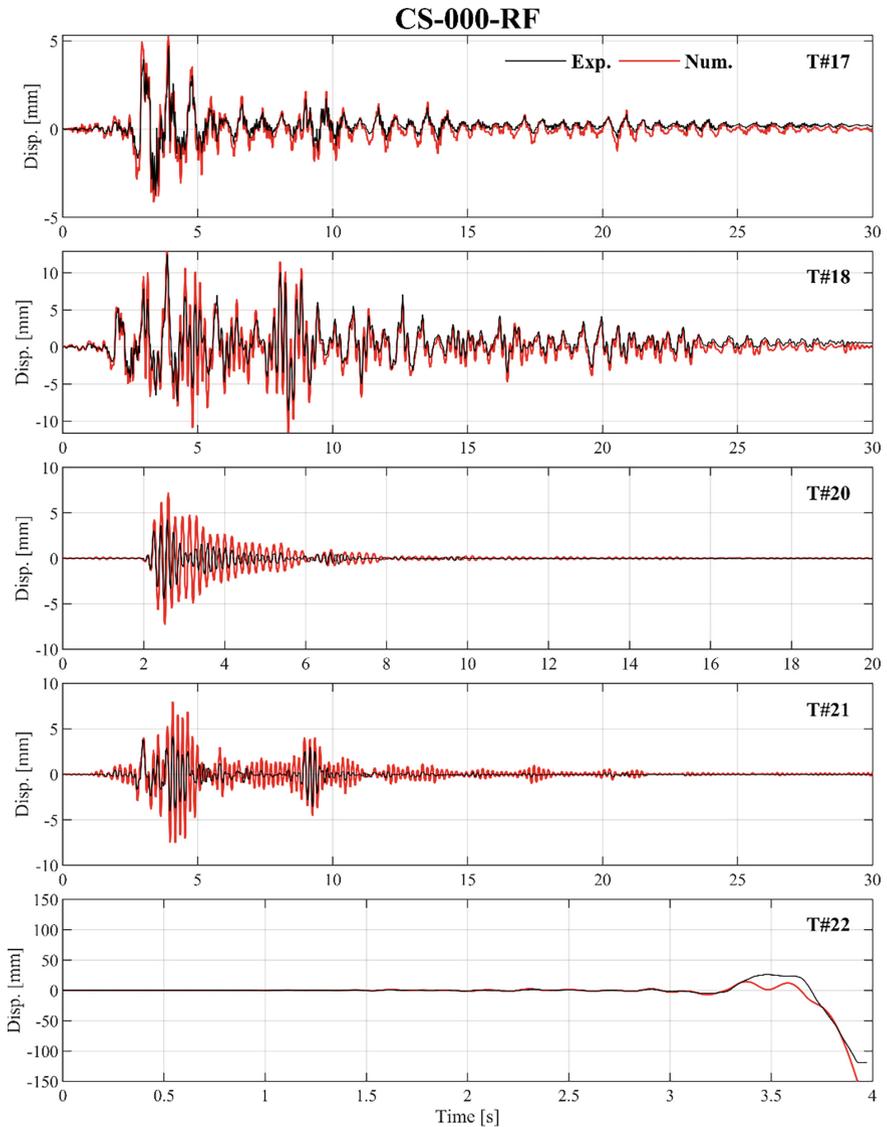
Fig. 4. Comparison of numerical and experimental displacement time histories for wall CS-000-RF

post-cracking phase. It is governed by ten parameters, which are effectively reduced to six independent parameters upon assuming an immediate phase transition. This transition is triggered once the wall's cracking resistance is exceeded. All model parameters can be analytically determined. The model demonstrates excellent agreement with incremental dynamic test outcomes, accurately depicting the progression from cracking to collapse not only for single leaf walls, but also in the case of cavity walls.
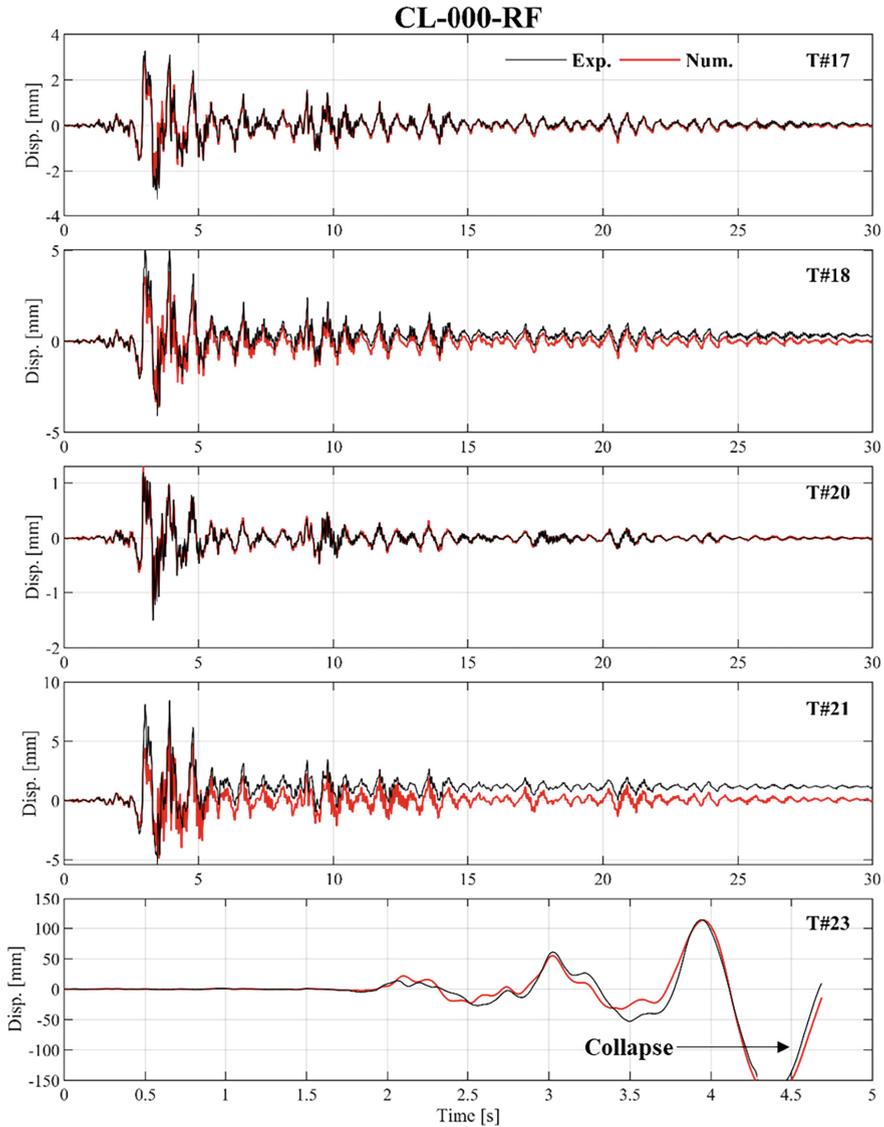
Fig. 5. Comparison of numerical and experimental displacement time histories for wall CL-000-RF

A promising avenue for future research suggested by this study involves comparing the seismic vulnerability of URM walls constructed with "Weak Unit-Strong Joint" (WU-SJ) masonry, characterised by vertical cracks traversing through the brick units and head joints under pure horizontal bending, against walls made of "Strong Unit-Weak Joint" (SU-WJ) masonry, where a stepped crack pattern is observed through head joints and
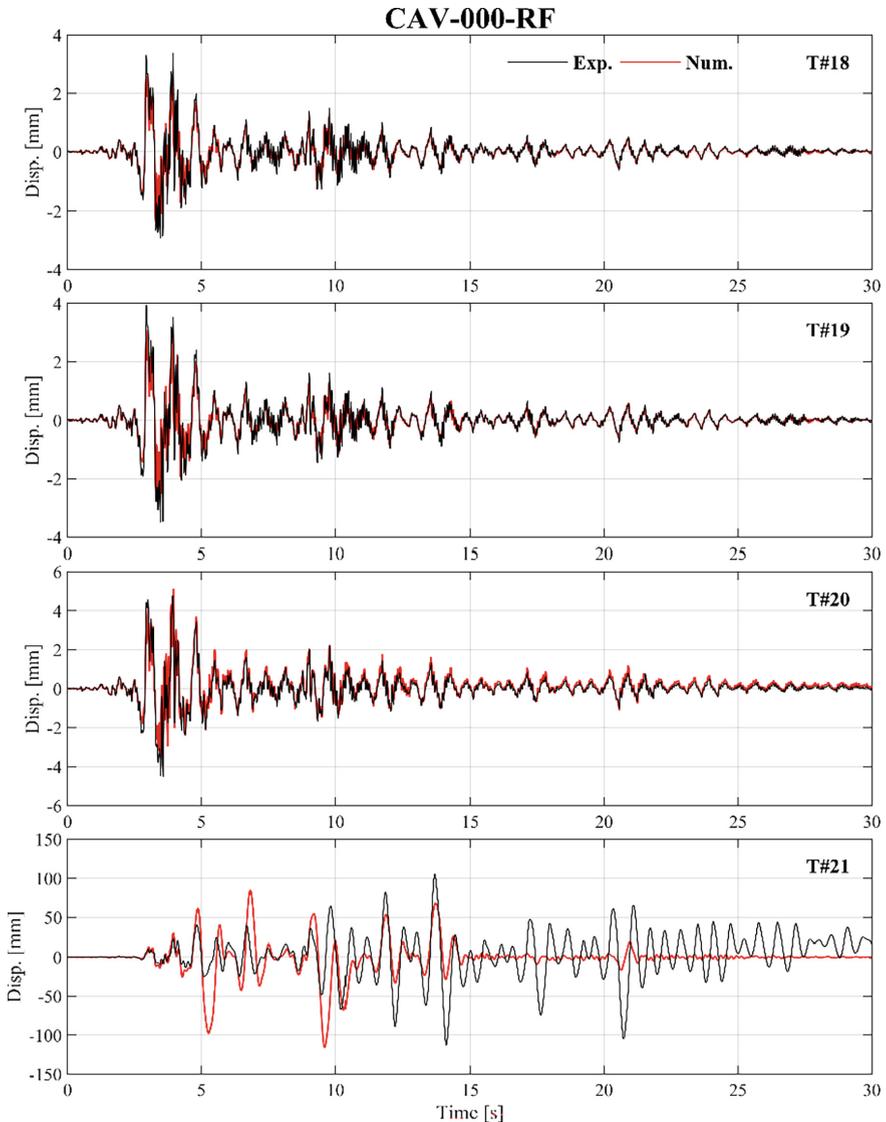
Fig. 6. Comparison of numerical and experimental displacement time histories for wall CAV-000-RF

half a bed joint under the same conditions. The model has simulated the dynamic out-of-plane two-way bending seismic behaviour of URM walls built using both specified masonry typologies, achieving good agreement with experimental findings. Similarly, an analysis comparing the vulnerability of cavity walls to that of single leaf walls would also be interesting.

References

1. Doherty K, Griffith MC, Lam N, Wilson J (2002) Displacement-based seismic analysis for out-of-plane bending of unreinforced masonry walls. Earthq Eng Struct Dyn 31:833–850. https://doi.org/10.1002/eqe.126
2. Lam NTK, Griffith M, Wilson J, Doherty K (2003) Time–history analysis of URM walls in out-of-plane flexure. Eng Struct 25:743–754. https://doi.org/10.1016/S0141-0296(02)00218-3
3. Sorrentino L, Masiani R, Griffith MC (2008) The vertical spanning strip wall as a coupled rocking rigid body assembly. Struct Eng Mech 29:433–453. https://doi.org/10.12989/sem.2008.29.4.433
4. Godio M, Beyer K (2019) Trilinear model for the out-of-plane seismic assessment of vertically spanning unreinforced masonry walls. J Struct Eng 145. https://doi.org/10.1061/(ASCE)ST.1943-541X.0002443
5. Graziotti F, Tomassetti U, Sharma S, Grottoli L, Magenes G (2019) Experimental response of URM single leaf and cavity walls in out-of-plane two-way bending generated by seismic excitation. Constr Build Mater 195:650–670. https://doi.org/10.1016/j.conbuildmat.2018.10.076
6. Sharma S, Tomassetti U, Grottoli L, Graziotti F (2020) Two-way bending experimental response of URM walls subjected to combined horizontal and vertical seismic excitation. Eng Struct 219:110537. https://doi.org/10.1016/j.engstruct.2020.110537
7. Vaculik J, Griffith MC (2017) Out-of-plane load–displacement model for two-way spanning masonry walls. Eng Struct 141:328–343. https://doi.org/10.1016/j.engstruct.2017.03.024
8. Jafari S, Rots JG, Esposito R, Messali F (2017) Characterizing the material properties of Dutch unreinforced masonry. Procedia Eng 193:250–257. https://doi.org/10.1016/j.proeng.2017.06.211
9. Rots JG, Messali F, Esposito R, Mariani V, Jafari S (2017) Multi-scale approach towards Groningen Masonry and induced seismicity. Key Eng Mater 747:653–661.https://doi.org/10.4028/www.scien-tific.net/KEM.747.653
10. Graziotti F, Penna A, Magenes G (2019) A comprehensive in situ and laboratory testing programme supporting seismic risk analysis of URM buildings subjected to induced earthquakes. Bull Earthq Eng 17:4575–4599. https://doi.org/10.1007/s10518-018-0478-6
11. Lawrence S, Marshall R (2000) Virtual work design method for masonry panels under lateral load. In: Porceedings of the 12th international brick/block masonry conference. Madrid, Spain
12. Council of Standards Australia (2001) AS 3700–2001: masonry structures. Australia, Sydney
13. NEN (2020) Assessment of structural safety of buildings in case of erection, reconstruction and disapproval–induced earthquakes–basis of design, actions and resistances. NPR9998+C1:2020
14. Willis C (2004) Design of unreinforced masonry walls for out-of-plane loading
15. Vaculik J (2012) Unreinforced masonry walls subjected to out-of-plane seismic actions
16. Sharma S, Graziotti F, Magenes G (2021) Torsional shear strength of unreinforced brick masonry bed joints. Constr Build Mater 275:122053. https://doi.org/10.1016/j.conbuildmat.2020.122053
17. Vaculik J, Griffith M (2008) Time-history analysis for unreinforced masonry walls in two-way bending. In: Proceedings of the 14th world conference of earthquake engineering. Beijing, China
18. Newmark NM (1959) A method of computation for structural dynamics. J Eng Mech Div 85:67–94. https://doi.org/10.1061/JMCEA3.0000098